THE JOURNAL OF BIOLOGICAL CHEMISTRY VOL. 290, NO. 42, pp. 25717–25727, October 16, 2015
Published in the U.S.A.

The Alternative Splicing of Cytoplasmic Polyadenylation Element Binding Protein 2 Drives Anoikis Resistance and the Metastasis of Triple Negative Breast Cancer*

Received for publication, June 10, 2015, and in revised form, August 20, 2015 Published, JBC Papers in Press, August 24, 2015, DOI 10.1074/jbc.M115.671206

Ryan M. Johnson[‡], Ngoc T. Vu[‡§], Brian P. Griffin[‡], Amanda E. Gentry[¶], Kellie J. Archer[¶‖], Charles E. Chalfant[‡ ‡‡§§¶¶‖‖‖1], and Margaret A. Park[‡ ‡‡2]**

*From the [‡]Department of Biochemistry and Molecular Biology, Virginia Commonwealth University, Richmond Virginia 23298, [§]Vietnam Education Foundation, Arlington, Virginia 22201, [¶]Department of Biostatistics, Virginia Commonwealth University, Richmond, Virginia 23298, [‖]Virginia Commonwealth University Massey Cancer Center Biostatistics Shared Resource, Richmond, Virginia 23298, **Center for the Study of Biological Complexity, Virginia Commonwealth University, Richmond, Virginia 23298, [‡‡]Virginia Commonwealth University Massey Cancer Center Massey Cancer Center, Richmond, Virginia 23298, [§§]Research and Development, Hunter Holmes McGuire Veterans Affairs Medical Center, Richmond, Virginia 23224, [¶¶]Virginia Commonwealth University Institute of Molecular Medicine, Richmond Virginia, 23298, and [‖‖]Virginia Commonwealth University Johnson Center, Richmond, Virginia, 23298*

Background: The acquisition of anoikis resistance (AnR) is an important mechanism in metastasis.
Results: AnR requires the up-regulation of the B isoform of CPEB2 via alternative RNA splicing (AS).
Conclusion: CPEB2 AS is a key mechanism in both AnR and the metastasis of breast cancer (BC).
Significance: Understanding the regulation of CPEB2 AS may lead to new targets for treatment of metastatic BC.

Triple negative breast cancer (TNBC) represents an anomalous subset of breast cancer with a greatly reduced (30%) 5-year survival rate. The enhanced mortality and morbidity of TNBC arises from the high metastatic rate, which requires the acquisition of AnR, a process whereby anchorage-dependent cells become resistant to cell death induced by detachment. In this study TNBC cell lines were selected for AnR, and these cell lines demonstrated dramatic enhancement in the formation of lung metastases as compared with parental cells. Genetic analysis of the AnR subclones *versus* parental cells via next generation sequencing and analysis of global alternative RNA splicing identified that the mRNA splicing of cytoplasmic polyadenylation element binding 2 (CPEB2), a translational regulator, was altered in AnR TNBC cells. Specifically, increased inclusion of exon 4 into the mature mRNA to produce the CPEB2B isoform was observed in AnR cell lines. Molecular manipulations of CPEB2 splice variants demonstrated a key role for this RNA splicing event in the resistance of cells to anoikis. Specifically, down-regulation of the CPEB2B isoform using siRNA re-sensitized the AnR cell lines to detachment-induced cell death. The ectopic expression of CPEB2B in parental TNBC cell lines induced AnR and dramatically increased metastatic potential. Importantly, alterations in the alternative splicing of CPEB2 were also observed in human TNBC and additional subtypes of human breast cancer tumors linked to a high metastatic rate. Our findings demonstrate that the regulation of CPEB2 mRNA splicing is a key mechanism in AnR and a driving force in TNBC metastasis.

Breast cancer is the second leading cause of cancer-related deaths in the United States. Although the 5-year survival rate for breast cancer is ~90%, triple negative breast cancer (TNBC;[3] *i.e.* cancers that are negative for the estrogen, progesterone, and EGF receptors) has a dramatically reduced (30%) 5-year survival rate. In addition, the secondary metastases characteristic of triple negative disease, not primary tumors, are the main cause of mortality. Hence, identification of novel targets, which play a role in the generation of circulating tumor cells, is of great importance for the development of new therapies to treat TNBC (1–3).

Regarding the mechanisms leading to cancer progression, a large number of processes are necessary and/or sufficient for the formation of distant metastases. These include invasion, epithelial to mesenchymal transition (EMT), anoikis resistance, intravasation, extravasation, arrest, and survival/proliferation in a distant organ (4). AnR, the process whereby cancer cells become desensitized to anchorage-dependent cell death, is an early and necessary step in the metastatic process for TNBC

* This work was supported, in whole or in part, by National Institutes of Health Grants HL125353 (to C. E. C.), CA154314 (to C. E. C.), 1R01LM011169 (to K. J. A.), 2P30 CA016059 (to K. J. A.), and T32 ES07334 (to K. J. A.), and K-series Award 8KL2TR000057-03 (to M. A. P.). This work was also supported by Veteran Affairs Merit Review I BX001792 (to C. E. C.) and a Research Career Scientist Award 13F-RCS-002 (to C. E. C.). The authors declare that they have no conflicts of interest with the contents of this article.

[1] To whom correspondence may be addressed: Dept. of Biochemistry and Molecular Biology, Sanger Hall, Rm. 2-016, Virginia Commonwealth University, Richmond, VA 23298. Tel.: 804-828-9526; E-mail: cechalfant@vcu.edu.
[2] To whom correspondence may be addressed: Dept. of Biochemistry and Molecular Biology, Sanger Hall, Rm. 2002b, Virginia Commonwealth University, Richmond, VA 23298. Tel.: 804-828-6594; E-mail: mpark4@vcu.edu.

[3] The abbreviations used are: TNBC, triple negative breast cancer; AS, alternative splicing; AnR, anoikis resistance or resistant; CPEB2, cytoplasmic polyadenylation element binding protein 2; EMT, epithelial to mesenchymal transition; poly-HEMA, poly(2-hydroxyethyl methacrylate); poly-HEMA, poly(2-hydrocyethylmethacrylate); RPKM, reads per kilobase per million; ANOVA, analysis of variance; TDAAC, Tissue and Data Acquisition and Analysis Core; VCU, Virginia Commonwealth University; Par, parental.

(3–5). Anoikis-resistant cells detach from the primary tumor and become circulating tumor cells, which arrest in a foreign organ and give rise to distant metastases. Indeed, a number of laboratories have used this process to study the mechanisms leading to metastasis (6, 7). Anoikis has also been linked by multiple groups to autophagy as well as multiple other signaling pathways including the EMT pathway, Notch signaling pathways, and STAT3 signaling pathways (8–12). Furthermore, cell signaling pathways regulating cell migration (ephrins; Ref. 13) and energy metabolism (osteopontin-c; Ref. 14) have also been linked to anoikis.

Some seminal studies have also been performed characterizing the influence of alternative splicing events in cancer development, cancer cell signaling, and EMT pathways. For example, CD44 alternative splicing, which has been linked to many cancers including breast cancer, has been shown to be regulated by splicing factors heterogeneous nuclear ribonucleoprotein M and ESRP1 (15–18). In another recent study, osteopontin-c and osteopontin-b isoforms were shown to be important in tumor progression (19). We have also demonstrated that caspase-9 alternative splicing (an event controlled by splicing factors heterogeneous nuclear ribonucleoprotein (hnRNP) L and hnRNP U) is integral to tumor formation/maintenance in lung cancer (20, 21). Regardless of these links between alternative splicing and cancer phenotypes, the role of alternative RNA splicing (AS) in the acquisition of AnR by TNBC cells has been overlooked.

In this study a novel link was discovered between the AnR of TNBC cells and the AS of cytoplasmic polyadenylation element binding protein 2 (CPEB2), a stress-activated regulator of polyadenylation, via the inclusion/exclusion of exon 4. This novel dysregulation of RNA splicing led to the increased expression of the functionally uncharacterized CPEB2 splice variant, CPEB2B, which we demonstrate is required for AnR, and thus, the metastatic capacity of TNBC cells. Therefore, this study has identified a new mechanism required for AnR that provides new insight into mechanisms associated with the metastasis of TNBC.

Experimental Procedures

Cell Culture and Reagents—The MDA-MB-231, MDA-MB-468, and BT549 cell lines (validated and purchased from American Type Culture Collection) were maintained in RPMI (Life Technologies). All cell lines were supplemented with 10% fetal bovine serum (Life Technologies) and 1% penicillin/streptomycin (Life Technologies). All cell lines were maintained in a 95% air, 5% CO_2 incubator at 37 °C. Cells were passaged once every 3–5 days (~90% confluence), and all experiments were performed during the first 12 passages. Antibodies were purchased from Cell Signaling with the exception of anti-CPEB2 (Santa Cruz Biotechnologies). Water soluble tetrazoium salt (WST) assay kits were purchased from Roche Applied Science. Annexin-V 7-aminoactinomycin D assay reagents were purchased from SouthernBiotech.

Selection of AnR Subpopulation of TNBC Cell Lines—To select for cells resistant to anoikis, poly(2-hydrocyethylmethacrylate) (poly-HEMA)-coated dishes (10 cm) were manufactured as in Sun *et al.* (9). Briefly, 4 ml of poly-HEMA (10 mg/ml) dissolved in 95% methanol, 5% sterile H_2O was allowed to evaporate from 10-cm dishes. Two coatings of poly-HEMA were applied. 1×10^7 MDA-MB-231 or MDA-MB-468 cells were then added to the poly-HEMA-coated dishes in normal media for a period of 3–5 weeks. Cell debris and cells killed by the detachment were eliminated by centrifugation every 3 days.

Plasmids and siRNA—Custom CPEB2A (NM_182646.2) and CPEB2B (NM_182485.2) constructs were made to our specifications using Celtek Genes service and then subsequent cloning into pcDNA3.1(+) vector. Custom siRNA molecules designed to down-regulate CPEB2A (5′-ACCCUUACAGGAUCGAAGUAGAAUGUAU-3′) or CPEB2B (5′-CAGCCGGAACAUCCAGAAUAGACCA-3′) were purchased from Sigma.

Transfection (Plasmid)—Plasmid transfections were accomplished using the Effectene system (Qiagen) according to the manufacturer's instructions. Briefly, plasmid DNA was incubated in the presence of DNA condensation buffer (EC buffer, supplied with the kit) and a 150:18 dilution of the Enhancer reagent for 10 min followed by the addition of the Effectene reagent (at a 168:20 dilution). Plasmid samples were incubated for a further 10 min then diluted to 1 ml with complete medium and added by single drops to the sample. Cells were allowed to accumulate the recombinant proteins for 24–48 h.

Transfection (RNAi)—Transfections were undertaken using the Amaxa Nucleofector kit V or Dharmafect reagent according to the manufacturer's instructions and as described previously (20–22).

Western Blotting—Total protein (10–20 μg) was electrophoretically separated on 7.5–10% polyacrylamide gels. Samples were transferred electrophoretically to PVDF membranes, then probed with the appropriate antibody as described previously (21, 22).

Quantitative Reverse Transcriptase-Polymerase Chain Reaction-PCR—Primer/probe sets were designed for CPEB2A (forward, 5′-GTGTTCAGAACAGACAACAATAG-3′; reverse, AATATCGATAAGGGAATTTTCC; Probe, 5′-CCCTTACAGGATCGAAGTAGAATGTATGACAG-3′) and CPEB2B (forward, 5′-CCTGGTCTATTCTGGATGTTCC-3′; reverse, 5′-ACCCTTACAGGTGAGATCTAGT-3′; probe, 5′-TCACTCCAAGATAGTTGGTGCACTGC-3′) and purchased from Integrated DNA Technologies. Quantitative reverse transcriptase-PCR was performed as described (20). cDNA was synthesized using the Superscript III kit (Life Technologies) and the manufacturer's instructions. Samples were then amplified using a Bio-Rad CFX Connect quantitative PCR machine and calculated using the standard curve method.

Quantitative Competitive RT-PCR—cDNA was synthesized using the Superscript III kit (Life Technologies) and the manufacturer's instructions. cDNA samples were subjected to traditional PCR as described (20–22) using the following primers located on either side of exon 4 of CPEB2B (forward, 5′-GTCCACAGAAGATGTTTATTTGATG-3′; reverse, 5′-CAATATCTGGAGGAAGACCACC-3) and an annealing temperature of 57 °C for 25 cycles. The resulting PCR samples were electrophoresed on 3.5% polyacrylamide gels in a Tris borate EDTA buffer system and stained with SYBR Gold according to the manufacturer's instructions. Gels were then imaged using a Typhoon 7000 imager (GE Healthcare). Densitometry was

performed using Image J, and ratios were determined for each sample. This ratio-based method is considered quantitative, as each splice variant acts as a competitive internal standard to the other variant (21, 22).

Survival Assays—Survival assays were undertaken as described previously (22). Briefly, single cells (150–300 cells per well) were plated onto 6-well plates. Plates were incubated 10–14 days to allow colonies to form. Colonies were stained with crystal violet, and colonies with >50 cells were counted.

Anoikis Resistance Assays—Cells were treated as indicated, then trypsinized, washed, and plated onto either normal (poly-lysine-coated) or poly-HEMA-coated plates. Cells were incubated an additional for 24 h and then stained with Annexin V-phycoerythrin and 7-aminoactinomycin D using the Apo-Screen Annexin V Apoptosis kit (Southern Biotech) according to the manufacturer's instructions. Cells were detected using a BD Biosciences FACSCanto II and analyzed using the accompanying FACSDIVA software as in West *et al.* (22).

Proliferation Assays—Proliferation was determined using a traditional WST assay (Roche Applied Science) according to the manufacturer's instructions. Briefly, cells (1×10^3) were plated onto each well of a 96-well plate. WST dye was added at 0-, 3-, and 5-day intervals and measured on a PerkinElmer Life Sciences Victor X3 plate reader at an absorbance of 450 nm.

Affymetrix Exon Array—The Affymetrix Expression Console software version 1.1 was used to evaluate the quality of the hybridizations and to process .CEL_les files. The robust multi-array average method for extended probe sets was used to obtain the probe set expression summary. For each probe set, a moderated *t* test was used to compare AnR *versus* parental samples using the limma Bioconductor package in the R programming environment. Probe sets having an false discovery rate < 0.10 were considered significant.

Next Generation Sequencing—FASTQ files used in this experiment can be found in the SRA database (Short Read Archives: PRJNA278375). The CLC Genomics Workbench was used to calculate transcript-level expression, which uses gene and mRNA-specific annotation for mapping reads against the gene and all known transcripts. Transcript-level expression values were reported as reads per kilobase per million (RPKM). Subsequently a linear regression model was used to regress the log transformed RPKM and identify differentially expressed transcripts as those outside the 95% prediction interval. All transcripts within the 95% prediction interval were retained as having equivalent expression. All transcripts with an RPKM < 1 were removed. To identify transcripts differentially expressed when comparing parental *versus* AnR samples, for each gene we summed the RPKMs over all transcripts to represent gene-level RPKM, which was used in calculating the proportion of transcript-specific expression, as the RPKM transcript/RPKM gene. The difference in proportion of transcript-specific expression was calculated. For each transcript included in the final analysis, a one-sample *t* test was performed to determine whether the difference in proportion of transcript-specific expression differed significantly from zero. A conservative *p* value of 0.05 was used in identifying transcripts having differential expression.

In addition to transcriptomic analysis, a secondary analysis was performed as follows (CASPER); TopHat version 2.0.9, in conjunction with Bowtie2 version 2.1.0, was used to align the four paired-end RNA-seq data to the human reference transcriptome and genome (UCSC hg19). Using the resulting bam files, cufflinks version 2.1.1 was used to assemble transcripts and estimate their abundances where we excluded reads from rRNAs and tRNAs by creating a mask file using UCSC Genome Browser. To identify differences between the AnR and parental samples, we tested for differential isoform expression in the two paired samples independently using Cuffdiff. The resulting isoform_exp.diff files that include transcript expression comparisons were read into the R programming environment. For within cell line comparisons, the *p* values were used to estimate the false discovery rate using the q-value method. Additionally, Fisher's method for combining *p* values was used to combine the *p* values across the two independent comparisons.

Analysis of Samples from The Cancer Genome Atlas (TCGA) Database—First, all breast cancer sample metadata were downloaded from the TCGA website (cancergenome.nih.gov). Samples were then divided into three categories (control, triple negative, and HER2-overexpressing). Samples not corresponding to either TNBC or HER2-overexpressing breast cancer were discarded. Samples were considered to be triple negative if they scored negative for estrogen, progesterone, and HER2 receptors and HER2 overexpressing if the samples scored a 2+ or above as determined by an *in situ* hybridization assay. Transcript-level text files were downloaded for the selected samples, and CPEB2A/CPEB2B ratios were determined using the RPKM values for these transcripts. Outliers and samples that had RPKM values of 0 for both CPEB2A and CPEB2B were discarded.

Murine Model of TNBC Metastasis—Female NOD scid gamma were allowed to acclimatize for 1–2 weeks. After acclimatization, 1×10^6 cells were resuspended in 10 μl of matrigel: collagen (1:1) and injected into the upper mammary fat pad of NOD scid gamma mice (The Jackson Laboratory) as in Rashid *et al.* (23, 24). Tumors were allowed to form for a period of 50–60 days. At morbidity (or after 60 days), mice were sacrificed, and both lungs and primary tumors were harvested for analysis. Animals that failed to develop primary tumors after 50 days were sacrificed and excluded from the study.

Biostatistics—Biostatistical analyses were performed using either SPSS or R. Statistical tests used include Student's *t* test (in the case of only two test conditions), ANOVA (in the case of multiple test conditions), the Mann-Whitney rank sum test (when normality fails, as in Fig. 2*D*), and an false discovery rate-adjusted *p* value (Benjamini-Hochberg correction) calculation (Cuffdiff).

Human Declaration of Approvals—All human tumor samples were de-identified and procured from the VCU Tissue and Data Acquisition and Analysis Core (TDAAC) under the approved IRB protocol number HM12702_Ame2. This resource has been approved by the VCU IRB in accordance to all United States rules and regulations and is housed in a Clinical Laboratory Improvement Amendments of 1988 (CLIA 1988) certified Molecular Diagnostics Laboratory in the VCU

Department of Pathology and the Virginia Commonwealth University Massey Cancer Center.

Animal Declaration of Approvals—Animal experiments were conducted at Virginia Commonwealth University. The research protocol was approved by the VCU IACUC involving animal care in accordance with the United States Department of Agriculture Animal Welfare Regulations, the Public Health Service Policy on the Humane Care and Use of Laboratory Animals, and the United States Government Principles for the Utilization and Care of Vertebrate Animals Used in Testing, Research, and Training (#AD10000529). VCU is in compliance with all provisions of the Animal Welfare Act and other federal statutes and regulations relating to animals. VCU is registered under the Animal Welfare Act as a class R research facility with the United States Department of Agriculture Animal and Plant Health Inspection Service (APHIS) Animal Welfare (registration number 52-R-0007). The Office of Laboratory Animal Welfare (OLAW) approved the VCU Animal Welfare Assurance in compliance with the Public Health Service Policy (assurance number A3281-01).

Results

Anoikis Resistance Enhances the Transformative Potential of Triple Negative Breast Cancer Cells—To examine the possible role of RNA splicing in AnR and the metastasis of TNBC, we first constructed AnR models of TNBC by isolating subclones of the TNBC cell lines MDA-MB-231 and MDA-MB-468. Specifically, MDA-MB-231 and MDA-MB-468 cells were chronically cultured on poly-HEMA-coated dishes. Poly-HEMA is a Teflon-like polymer that when applied to tissue culture dishes prevents cells from adhering to the surface. Exposing cells to dishes coated with this polymer, therefore, led to the selection of cells resistant to anoikis, which propagated independent of attachment (Fig. 1*A*). These AnR subclones of MDA-MB-231 and MDA-MB-468 demonstrated significant enhancement of cellular phenotypes associated with higher tumorigenic capacity and metastatic potential. Specifically, these AnR subclones demonstrated dramatically increased phosphorylated focal adhesion kinase (*FAK*, Fig. 1*B*), enhanced cell survival/colony formation (Fig. 1*C*), and enhanced proliferation (Fig. 1*D*). Although the survival/colony formation and proliferation assays are indicators of transformation/metastatic potential, a more accurate assessment of metastatic potential requires an animal model. We, therefore, injected cells into the upper mammary fat pad of NOD scid gamma mice and observed metastatic tumor formation in the lungs of these mice. Importantly, the AnR subclones, when implanted into the upper mammary fat pad, formed dramatically higher numbers of lung metastases as well as larger primary tumors than the parental control cell lines (Fig. 1, *E* and *F*). Taken together, these results demonstrate that the sensitivity of TNBC cells to anoikis is linked to metastatic ability.

Next Generation Deep RNA Sequencing Identifies a Common Dysregulated Splicing Event Associated with AnR—Recently, mRNA processing via alternative RNA splicing has been implicated as an important set of events in tumor progression (16, 17, 20, 21). Therefore, we used both next generation RNA sequencing (using both MDA-MB-231 and MDA-MB-468 parental (Par) and AnR cell lines) and traditional exon array (using MDA-MB-231 Par and AnR only) technologies to first interrogate the global set of AS events dysregulated during the acquisition of AnR (Fig. 2*A*). A total of 268 AS events were identified as altered using a combination of transcriptomic and CASPER analysis in AnR MDA-MB-231 and AnR MDA-MB-468 cell lines as compared with their respective Par cell lines. Comparing these 268 AS events to the 1931 AS events altered in AnR MDA-MB-231 cells *versus* Par, as determined via traditional exon array, alterations in 62 AS events were identified by both approaches as linked to AnR. A Venn diagram of genes found to be differentially regulated using both technologies and in both cell lines is shown in Fig. 2*B*. The list of 62 genes was further revised by first determining which genes had isoforms that were oppositely regulated as an indication of an alternative splicing event instead of the entire gene being up- or down-regulated (Fig. 2*C*). These data indicate that a subset of 18 AS events are altered in an opposing fashion in AnR TNBC cells.

To determine AS events to further interrogate for a mechanistic role in AnR, two criteria were required: 1) the alteration in AS is confirmed by competitive RT-PCR in AnR TNBC cells *versus* parental, and 2) the altered AS event is observed in human TNBC. In this regard the AS of CPEB2 was the only AS event confirmed under these criteria (data not shown). For this AS event, next generation RNA sequencing demonstrated that AnR TNBC cells demonstrated a significant loss in the CPEB2A variant (−exon4) with a concomitant increase in CPEB2B (+exon4) as compared with parental TNBC cells (Fig. 3*A*). Thus, PCR primers surrounding exon 4 were designed, and Par and AnR cDNA was further analyzed using competitive RT-PCR (Fig. 3*B*) to confirm splicing dysregulation by AnR development, and a significant decrease in the ratio of CPEB2A/B mRNA, corresponding to an increase in the CPEB2B isoform, was observed in AnR TNBC cell lines as compared with parental TNBC cell lines (Fig. 3*B*). Fig. 3*B* also demonstrated that CPEB2 is not aberrantly spliced in the non-tumorigenic cell line MCF10A, as the only band visible corresponds to CPEB2A. Furthermore, parental MDA-MB-468 cells, which already possessed moderate AnR and enhanced metastatic potential (Fig. 1*E*), demonstrated dysregulated CPEB2 RNA splicing in favor of CPEB2B expression as compared with MCF10A and MDA-MB-231 parental cells (Fig. 3*B*). The identity of the CPEB2 isoforms was confirmed by gel extraction of the PCR fragments followed by DNA sequencing, which verified that CPEB2A excludes 90 nucleotides corresponding to exon 4 of the CPEB2B gene (nucleic acids 1944–2034; data not shown and Refs. 25–28). The CPEB2B isoform is a recently discovered one that was partially characterized in murine models earlier this year (25–28). These data demonstrate that aberrantly spliced CPEB2 pre-mRNA produces the splice variant of CPEB2, CPEB2B, which is strongly associated with AnR in TNBC.

To validate our second criterion for CPEB2 AS, a panel of 15 breast cancer tumors with patient-matched control (tumor adjacent) breast tissue was examined for CPEB2 mRNA splicing (Fig. 3*C*). Indeed, human breast cancer tumors patient-matched to control tissues demonstrated a dramatic decrease in the CPEB2A/B ratio similar to the CEPEB2A/B mRNA ratio observed in the AnR cell lines. Because these tumor samples

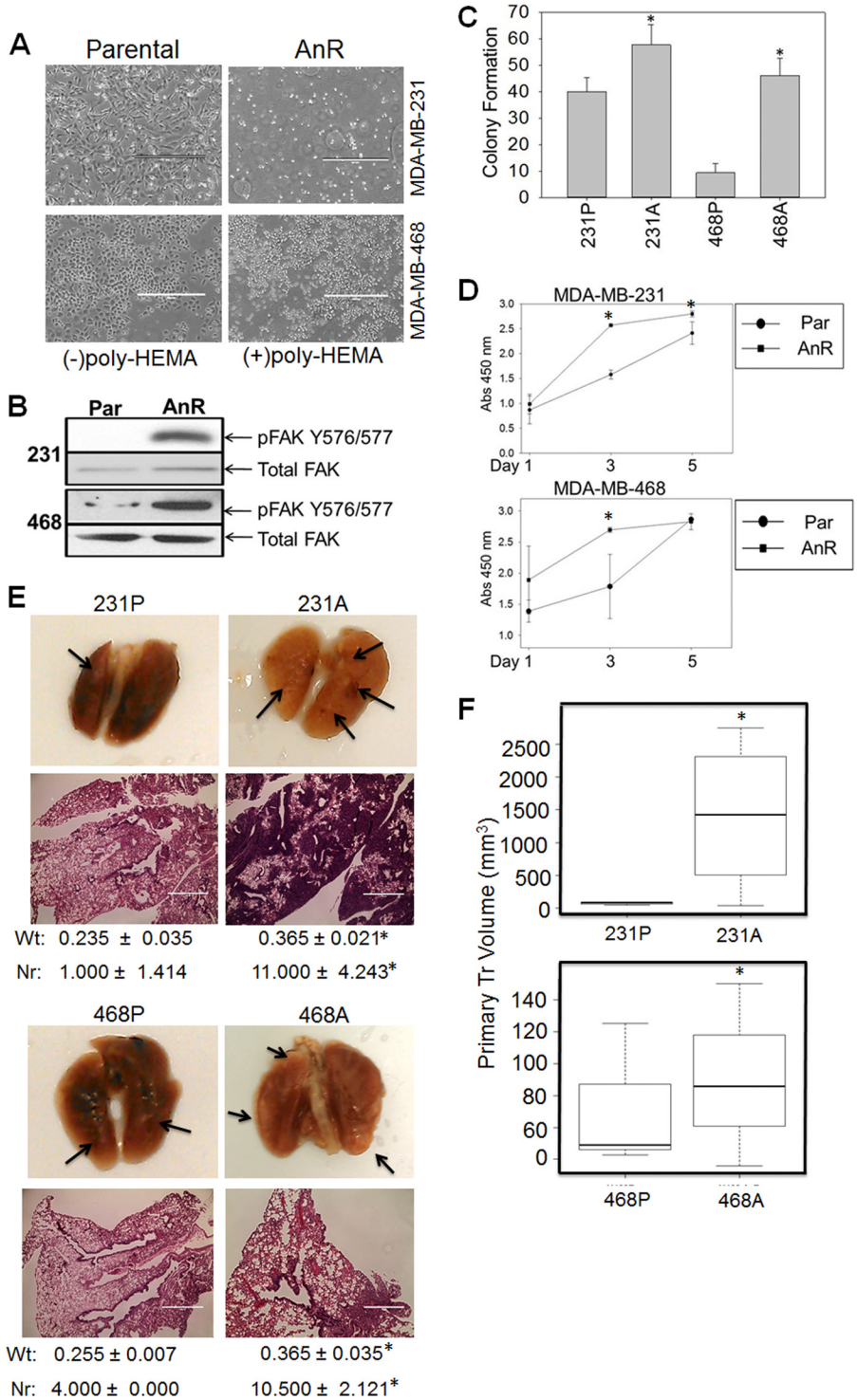

FIGURE 1. **Development of anoikis resistance models of metastasis for TNBC.** *A*, the AnR populations of MDA-MB-231 and MDA-MB-468 cells were isolated by selection on poly-HEMA-coated plates and micrographed (*scale bar* = 1 μm). *B*, total protein was isolated from Par and AnR MDA-MB-231 and MDA-MB-468 cells and subjected to SDS-PAGE followed by analysis by Western immunoblot for phosphorylation of focal adhesion kinase (*FAK*) on Tyr-576/577, a cellular marker of AnR. *C* and *D*, cell survival (*C*) and proliferation (*D*) of Par and AnR cells were determined via clonogenic assay and MTT (3-(4,5-dimethylthiazol-2-yl)-2,5-diphenyltetrazolium bromide) assay as described (20–22) ($n = 6$). *E* and *F*, TNBC cells (1×10^6) were injected into the T1 fat pad of NOD scid gamma mice ($n = 6$). After 50–60 days, primary tumors were measured via caliper (*F*), and lungs (pictured in *E*, *top pictures*) were harvested and analyzed for weight (*Wt*) and number of metastases (*Nr*) and stained with H&E (*bottom micrographs*). *Arrows* indicate lung metastases. * indicates a statistically significant difference from control/parental (ANOVA or *t* test, $p < 0.05$).

were not confirmed TNBC, but may have represented other subtypes, we then analyzed a larger set of 45 TNBC-specific tumor tissues. We compared the CPEB2A/B ratio of the TNBC tissues to the control tissues analyzed in Fig. 3*C* (Fig. 3*D*). Finally, an experiment was undertaken to query the results from The Cancer Genome Atlas (TCGA) database (cancergenome.nih.gov). Next generation sequencing results were downloaded along with clinical data. The levels of CPEB2A and

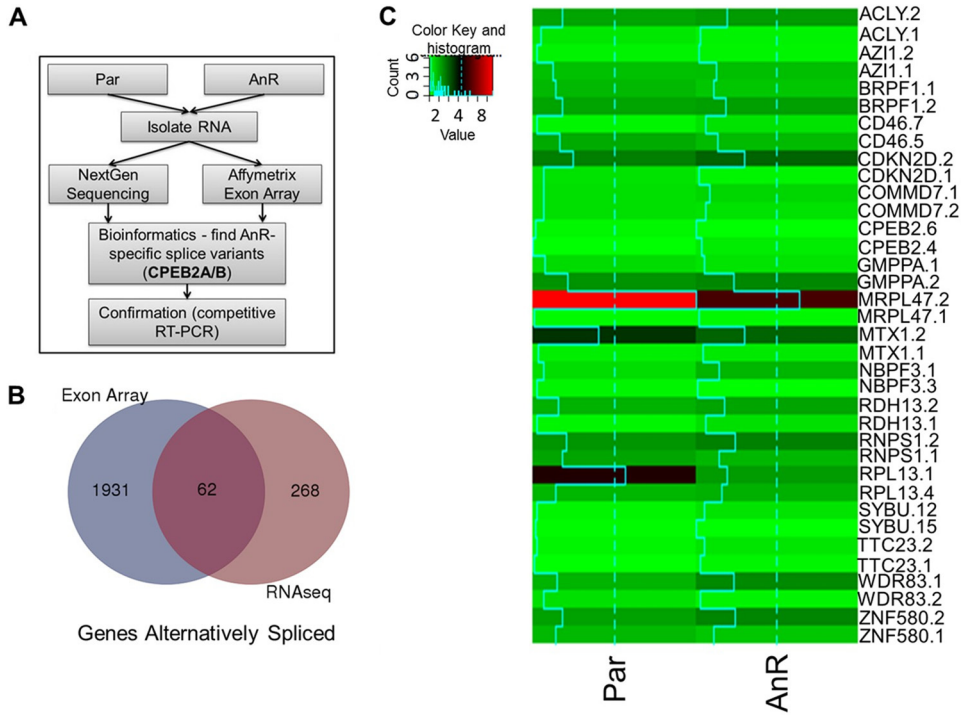

FIGURE 2. **Alternative RNA splicing is altered in AnR TNBC cells *versus* Par TNBC cells.** *A*, overview of double RNA sequencing and exon array screen for alternative RNA splicing variations during the selection of TNBC cells for AnR. *B*, Venn diagram showing the overlap between the two types of screen (nextgen sequencing (*purple*) and exon array (*blue*)). 62 genes were found to be dysregulated. *C*, heatmap of the 18 alternatively spliced variants (36 transcripts in all) identified in both MDA-MB-231 and MDA-MB-468 Par *versus* AnR cell lines from the 62 AS events identified in *B*. Data represent the average difference between the MDA-MB-231 cell lines.

CPEB2B in normal control samples and samples that scored negative for the estrogen, progesterone, and HER2 receptors were analyzed (Fig. 3*E*), and a statistically significant decrease was observed for the CPEB2A/B mRNA ratio in TNBC *versus* normal tissue. To determine whether the dysregulation of CPEB2 AS translates to additional subtypes of breast cancer with high metastatic rates, next generation sequencing data from Her2-overexpressing breast cancer were analyzed for CPEB2 RNA splicing and found to be significantly different from control samples. In sum, these results demonstrate that a low ratio of CPEB2A/CPEB2B mRNA is linked to AnR and observed in human TNBC as well as additional subtypes of breast cancer linked to higher mortality and metastatic rates (*i.e.* Her2-overexpressing breast cancers).

Human CPEB2 Splice Variants Have Opposing Effects on Anoikis Resistance and Metastasis—In the next set of studies, we first confirmed that the isoforms of CPEB2 were translated to the protein level. Using a CPEB2 antibody raised against the entire protein, a significant increase in the ~75-kDa band (*i.e.* CPEB2B), and a decrease in the ~65-kDa form of CPEB2 (*i.e.* CPEB2A) was observed in both AnR MDA-MB-231 and AnR MDA-MB-468 cells *versus* parental cell lines (Fig. 4, *A* and *B*). Because these isoforms have never been systematically studied, we needed to ensure that these protein bands correspond to CPEB2A and -B. Therefore, siRNAs specific to each CPEB2 splice variant were designed. siRNA sequences specific to the exon3-exon5 junction (CPEB2A-specific) and siRNAs specific to the internal exon 4 sequence (CPEB2B-specific) were designed and tested using quantitative PCR. Indeed, both quantitative reverse transcriptase-PCR and immunoblotting indicated that the appropriate CPEB2 splice variant was specifically down-regulated by this siRNA approach (Fig. 4, *C* and *E*). These data further demonstrated that the expression of CPEB2B protein is greatly enhanced in AnR TNBC cells along with a concomitant reduction in CPEB2A as compared with parental controls.

Using this molecular approach to specifically manipulate the expression of the CPEB2A and -B splice variants, the function of the individual splice variants on AnR was then examined. The "gold standard" for assaying AnR is to plate the cells of interest onto an attachment-resistant surface and measure apoptosis. We used poly-HEMA-coated plates to achieve an attachment-resistant surface and used polylysine-coated surfaces as a control. Down-regulation of CPEB2B (+exon4) in the AnR MDA-MB-231 cells alleviated the AnR phenotype of these cells with the percentage of cell death via anoikis similar to parental cells. Interestingly, the down-regulation of CPEB2B in Par MDA-MB-231 cells increased cell death via anoikis an additional 25%. (Fig. 4, *D* and *F*). Intriguingly, specific down-regulation of CPEB2A (−exon4) enhanced resistance to anoikis in Par MDA-MB-231 cells (Fig. 4, *D* and *F*) but not AnR MDA-MB-231 cells. These effects were also observed in MDA-MB-468 cells (Fig. 4, *E* and *G*).

Using a contrasting molecular approach, parental cell lines that stably express either CPEB2A or CPEB2B were developed (Fig. 5, *A* and *B*). Ectopic expression of CPEB2A decreased AnR, and in stark contrast, ectopic expression of CPEB2B induced AnR in parental TNBC cells (Fig. 5*C*). siRNA targeted against the ectopically expressed isoform "rescued" the observed effects demonstrating phenotypic specificity for the ectopically

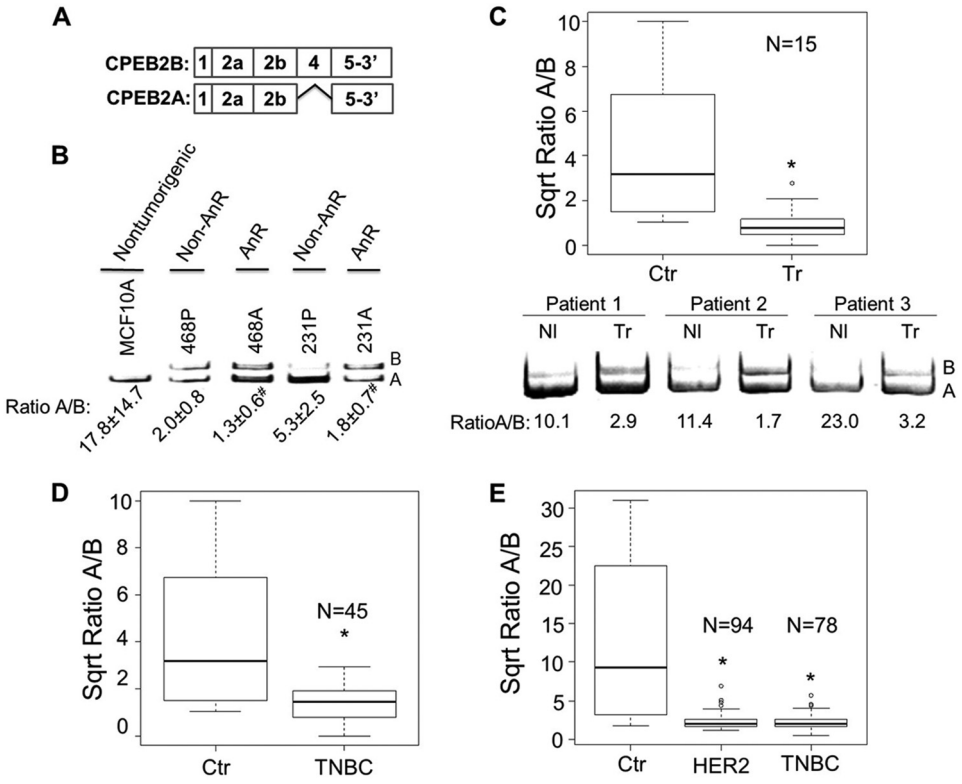

FIGURE 3. **CPEB2 splicing is altered in AnR TNBC cells and in human breast cancer tissues.** *A*, schematic representation of the experimentally confirmed CPEB2 splice variants associated with AnR in TNBC cells. *B*, RNA was isolated from the cell lines indicated, then first-strand cDNA synthesis was performed. cDNA samples were subjected to quantitative competitive RT-PCR and electrophoresed on a 5% acrylamide gel to determine the CPEB2A/B ratio (the presented gel is a representative of at least three different experiments; # indicates a statistically significant difference between parental and AnR cell lines (MDA-MB-468 and MDA-MB-231, *t* test, $p \leq 0.05$)). *C*, human breast tumor (*Tr*) and patient-matched normal control (*Nl* or *Ctr*) tissue was harvested, and RNA was isolated by the TDAAC. cDNA was synthesized, and samples ($n = 15$ for both control and tumor) were subjected to first strand cDNA synthesis and then quantitative PCR (*top graph; Sqrt Ratio A/B*, the square root of the ratio of the A isoform divided by the B isoform). A subset of three patient samples with matched controls was subjected to competitive RT-PCR (bottom gel). *D*, confirmed human TNBC tumor tissues ($n = 45$) obtained by the TDAAC were compared with the control patient tissues described in *C* using quantitative reverse transcriptase-PCR. *E*, transcript RPKM data for control samples ($n = 4$), HER2-overexpressing samples ($n = 94$), and TNBC samples ($n = 78$) were downloaded from the ATLAS cancer genome archive. The ratio of CPEB2A/CPEB2B was determined as described under "Experimental Procedures." Outliers and samples for which CPEB2A and -B mRNA levels were both 0 were not considered. CPEB2A/B ratios from competitive RT-PCR experiments were determined using ImageJ. * indicates a statistically significant difference from non-tumor cells (Mann-Whitney, $p \leq 0.05$).

expressed cDNA (Fig. 5*D*). Importantly, the BT549 TNBC cell line, which failed to acquire AnR after Poly-HEMA selection, was able to survive independently of attachment after forced expression of CPEB2B (Fig. 5, *E* and *F*). These data show that AS of CPEB2 plays a major role in AnR with the splice variants of the CPEB2 gene, CPEB2A and -B, having opposing roles in the sensitivity of TNBC cells to anoikis.

Based on the above findings with anoikis, we next examined the role of these CPEB2 splice variants in enhancing/decreasing the metastatic capacity of MDA-MB-231 parental cells. Par MDA-MB-231 cells stably overexpressing CPEB2A or CPEB2B were implanted into the upper mammary fat pad of NOD scid gamma mice as in Fig. 1. Sixty days later, lung metastases and primary tumor size were assessed. Stable overexpression of CPEB2B induced a dramatic increase in lung metastases (Fig. 5, *G* and *H*). To further confirm the role of CPEB2B in driving TNBC metastasis, we stably expressed CPEB2B shRNA in the AnR MDA-MB-231 cell line. Intriguingly, specific down-regulation of CPEB2B led to complete loss of clonogenicity for these AnR cell lines (data not shown). Taken together, these data demonstrate that CPEB2 splice variants have major roles but opposing functions in both AnR and TNBC metastasis. In particular, CPEB2B expression is a requirement for the acquisition of AnR, survival of AnR TNBC cells, and the subsequent efficient metastasis of these TNBC cells. Overall, our data have identified a novel and important splicing event in the metastatic process.

Discussion

A full understanding of the metastatic process is crucial to the future eradication of lethal TNBC via a new generation of therapeutics. In this regard we have discovered a previously undescribed mechanism driving the acquisition of AnR and subsequent metastasis of TNBC cells. Specifically, we found that an alteration in the alternative RNA splicing of CPEB2 to express the CPEB2B splice variant coincides with the phenotype of AnR. More importantly, we showed that this event was required for selection of AnR TNBC cells, and thereafter the expression of the CPEB2B isoform was shown to be sufficient to induce AnR in TNBC cells as well as dramatically enhance the metastatic potential of these cells. This altered mRNA splicing was also observed in human TNBC as well as in an additional subtype of breast cancer associated with higher mortality and metastatic rates, ErbB2-overexpressing breast cancer. Hence,

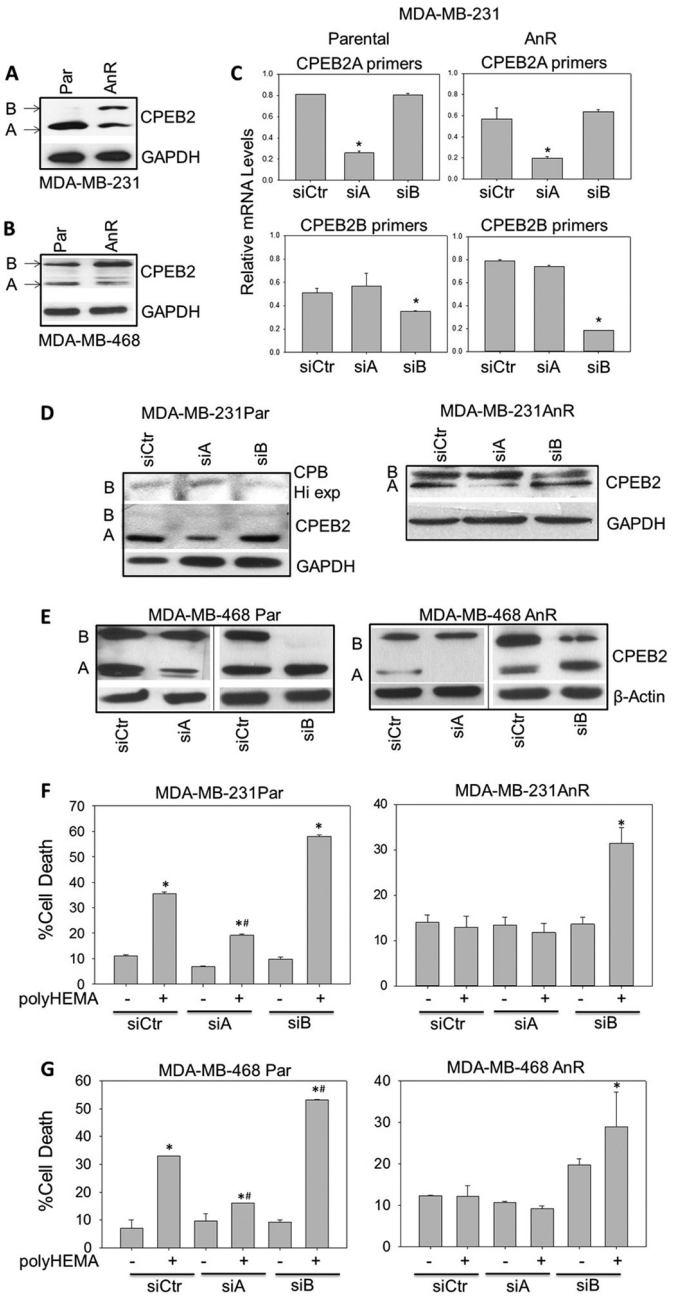

FIGURE 4. **CPEB2 isoforms have opposing functions in AnR.** Total protein from MDA-MB-231 (*A*) and MDA-MB-468 (*B*) cells was subjected to Western immunoblotting for CPEB2. *C* and *E*, siRNA was designed against either the CPEB2 exon 4 splice junction (CPEB2A-specific siRNA) or internally to exon 4 of CPEB2 (CPEB2B-specific siRNA) and tested in MDA-MB-231 Par and AnR cells via quantitative PCR (*C*) or both MDA-MB-231 and MDA-MB-468 Par and AnR cells via Western immunoblotting (*D* and *E*). Of note, Par MDA-MB-231 cells do not express CPEB2B at high levels. Therefore, a high exposure of CPEB2B was required (labeled *CPB Hi exp*)) to observe the effect of CPEB2B-specific siRNA. *F* and *G*, MDA-MB-231 or MDA-MB-468 Par (*left*) or AnR (*right*) cells were assayed for anoikis (detachment-induced apoptosis) after "knockdown" of the indicated CPEB2 isoform. Anoikis was assayed using the Apo-Screen Annexin V Apoptosis kit and a BD Biosciences FACSCanto II. * indicates a statistically significant difference from control/parental cells (ANOVA, $p < 0.05$). # indicates a statistically significant difference from the parental cells cultured under the poly-HEMA-coated condition (ANOVA, $p < 0.05$).

these findings lead us to speculate that CPEB2B expression is crucial for a highly aggressive phenotypes observed for these subtypes of breast cancer. Thus, this study has identified a completely novel mechanism driving metastasis of breast cancer cells.

As for the function of CPEB2 in regulating the resistance of TNBC cells to anoikis, McKnight and co-workers (29) have shown that CPEB2 is a regulator of cellular stress responses. Specifically, this group showed that CPEB2 is localized to RNA stress granules via a "low complexity sequence" where the factor binds to the mRNA of specific transcripts. This interaction of CPEB2 maintains these transcripts in an inactive state and is not translated until a stress is encountered. In response to stress, CPEB2 dissociates from the target transcript and allows the polyadenylate tail to elongate and/or alternative polyadenylation sites to be used followed by subsequent translation of the mRNA by the ribosomal complex (29–33). Two such mRNA transcripts reported to be regulated by CPEB2 are HIF1α and TWIST1 (25–28), factors strongly associated with cancer progression and the EMT. As we show that CPEB2A sensitizes TNBC cells to anoikis, one can hypothesize that CPEB2A is the specific isoform of CPEB2 acting as an inhibitor of HIF1α and TWIST1 polyadenylation and translation, As we also observed a previously unknown antagonism between the two CPEB2 splice variants, CPEB2A and -B, we can further hypothesize that CPEB2B has the opposing function. Indeed, before this study, a functional role specifically for any CPEB2 splice variant/isoform had not been shown or surmised. Thus, these hypotheses warrant future investigation, and it is enticing to surmise that the regulation of this splice mechanism is a key mechanism in regulating cellular stress responses in general.

If CPEB2A and -B play antagonistic roles in regulating the polyadenylation and translation of the same RNA transcripts, several possible mechanisms can be postulated. For example, both CPEB2A and -B retain their RNA binding domains, and thus, a simple, competition-based antagonism for the interaction of these factors with specific RNA *cis* elements is a likely possibility (34, 35). What is less clear is how the inclusion of 30 amino acids in full-length CPEB2B upstream of one of the RNA binding domains would completely alter the regulatory function of this factor. Indeed, we do not know whether one or both splice variants are localized to stress granules, but CPEB2B may simply function to bind specific mRNAs and block them from associating with CPEB2A and stress granules, which thereby allows alternative polyadenylation and translation. Another mechanistic explanation may be that the inclusion of the additional 30 amino acids changes the structure of CPEB2B so that the factor now presents the bound RNA for efficient polyadenylation *versus* inhibiting the polyadenylation when bound to CPEB2A. Regardless, additional cellular and structure/function studies are required to elucidate this exciting new mechanism. This study may pave the way for novel discoveries determining how RNA splicing is a key upstream regulator of stress pathway by affecting the ability of CPEB2 factors to inhibit polyadenylation.

Because CPEB2 RNA splicing can be postulated to act as an upstream regulator of stress responses, the temporal nature and specificity of the mechanisms regulating this splicing event also become important. There are a number of reports over the last two decades demonstrating that alternative RNA splicing can be regulated in a rapid and acute manner in response to extra-

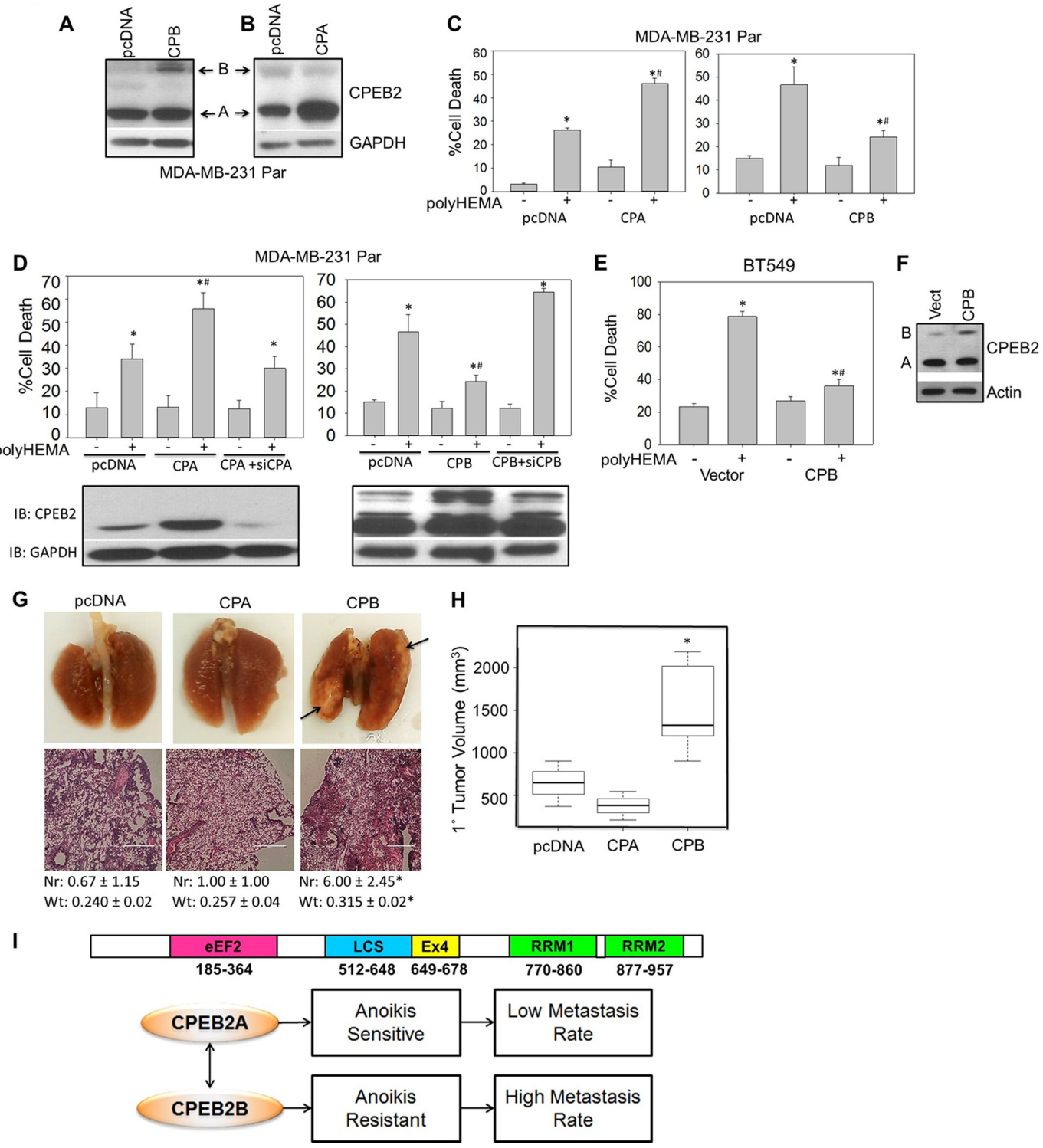

FIGURE 5. **CPEB2B expression induces AnR and enhances TNBC metastasis.** *A* and *B*, Western immunoblots of Par MDA-MB-231 genetically manipulated to ectopically express either CPEB2B (*A*) or CPEB2A (*B*). *C*, CPEB2A (*left graph*) or CPEB2B (*right graph*) overexpressing MDA-MB-231 Par cells were plated onto poly-HEMA-coated plates, and 24 h later these cells were assayed for detachment-induced cell death (*i.e.* anoikis) as in Fig. 4, *F* and *G*. *D*, CPEB2A (*left graph*) or CPEB2B (*right graph*) overexpressing cells were subjected to siRNA rescue of CPEB2A or CPEB2B levels as indicated. After 48 h exposure to siRNA (*lower blots*), cells were plated onto poly-HEMA-coated plates and assessed for anoikis (*upper graphs*). *IB*, immunoblot. *E* and *F*. BT549 cells were stably transfected with CPEB2B (F) and subsequently assayed for AnR. *G* and *H*, MDA-MB-231 cells stably expressing the indicated isoform of CPEB2 (1×10^6) were injected into the upper mammary fat pad of NSG mice as described in Fig. 1. 40–50 days later lungs (*G*) were harvested, and the weight (*Wt*) and number (*Nr*) of visible metastases were determined. Primary tumor volume was determined and are presented in *H*. *I*, structure of the CPEB2 protein. Amino acids numbered from the N terminus are indicated (*upper*), and the outline of hypothetical CPEB2 A and B function (*lower*) is shown. *Arrows* indicate lung metastases. * indicates $p < 0.05$ compared with polylysine-coated conditions or control cells (ANOVA or Mann-Whitney). # indicates $p < 0.05$ compared with stable overexpression of vector control (ANOVA).

cellular agonists. For example, both the alternative splicing of the insulin receptor and protein kinase Cβ (PKCβ) are manipulated within minutes by growth factors, which for PKCβ alternative splicing was functionally significant in terms of insulin-stimulated glucose uptake (37, 38). Hence, it is possible that an external stress can induce a rapid change in CPEB2 RNA splicing and thereby induce the expression of CPEB2B and acutely drive stress responses. Thus, this study may have defined a key "upstream" regulatory mechanism in regard to stress responses such as the hypoxic response, which may be "hijacked" by oncogenic factors linked to metastasis.

In relation to oncogenic factors, there are a number of reports on RNA splicing factors acting as oncogenes via either increased expression or via post-transcriptional modifications. For example, SRp30a (SRSF1) was shown to be a proto-oncogene and up-regulated in a large percentage of breast cancers (39–41). This factor has also been shown to be hyperphosphorylated in lung cancer cells, which is linked to the alternative splicing of caspase 9 and cancer phenotypes such as anchorage-independent growth, chemotherapy resistance, and tumor formation (42, 43). The expression of a number of RNA splicing factors is also linked to tumor progression in various cancers and cancer phenotypes. For example, Carstens and co-workers (15) have also linked the expression of two RNA *trans*-factors, ESRP1 and -2, in driving the EMT in cancer cells. Whereas preliminary studies via a small scale siRNA screen suggest that ESRP1 is not mediating the alternative splicing of CPEB2 (data not shown), we have not "ruled out" SRSF1 or ESRP2 in driving AnR via CPEB2 RNA splicing.

In relation to the regulatory mechanism for CPEB2 RNA splicing, it was intriguing that we were unable to select a subpopulation of BT549 that was AnR via poly-HEMA, whereas forced expression of CPEB2B readily induced AnR in these cells. Although there may be a number of possible explanations, our study suggests that the RNA *trans*-factors or upstream cell signaling pathways driving the inclusion of exon 4 into the mature CPEB2 transcript is not activated by detachment-induced cell stress or dysfunctional in these cells. Supporting this supposition, BT549 cells, although triple negative, are molecularly and functionally distinct from other TNBC cell lines used in this study. For example, BT549 cells overexpress androgen receptor and hyperphosphorylate both Akt and EGFR, in contrast to MDA-MB-231 cells (35). In addition, these cells do not seem to form tumors in mice (36), suggesting that a particular signaling pathway required for this cancer phenotype is not active, which may also be required to induce the inclusion of exon 4 into the CPEB2 transcript. Hence, the identification of the RNA splicing mechanism or oncogenic mutations linked to CPEB2 expression may provide insight into how AnR is acquired by TNBC and possibly other aggressive subtypes of breast cancer.

In conclusion, we have identified an important splicing event linked to AnR, a necessary first step in the metastatic process of TNBC. The ability of CPEB2 expression to induce AnR in TNBC broadly translated to additional TNBC cell lines. Alterations in CPEB2 RNA splicing were also observed in human TNBC. Although future mechanistic and preclinical studies are required, this study suggests that direct inhibition of CPEB2B or inhibition for the RNA splicing factor regulating the inclusion of exon 4 may suppress the metastasis of TNBC.

Author Contributions—Conception and design was by C. E. C. and M. A. P. Development and methodology was designed by R. M. J., M. A. P., A. E. G., and N. T. V. Acquisition of data was by R. M. J., A. E. G., M. A. P., B. P. G., and N. T. V. Analysis and interpretation was by K. J. A., C. E. C., and M. A. P. Writing and review of the manuscript was by K. J. A., C. E. C., and M. A. P. Study supervision and design was by M. A. P.

Acknowledgments—Services (Biostatistics Shared Resource Core, Flow Cytometry Shared Resource Core, TDAAC) and products in support of the research project were generated by the VCU Massey Cancer Center supported, in part, with funding from NCI, National Institutes of Health Cancer Center Support Grant P30 CA016059. We acknowledge Dr. Jenn Mietla and Dr. L. Alexis Hoeferlin for tireless efforts in editing this manuscript. In addition, we acknowledge Dr. Kazuake Takabe for great help with interpreting lung metastasis data.

References

1. Schmadeka, R., Harmon, B. E., and Singh M. (2014) Triple-negative breast carcinoma: current and emerging concepts. *Am. J. Clin. Pathol.* **141,** 462–477
2. Lehmann, B. D., Bauer, J. A., Chen, X., Sanders, M. E., Chakravarthy, A. B., and Shyr, Y. (2011) Identification of human triple-negative breast cancer subtypes and preclinical models for selection of targeted therapies. *J. Clin. Invest.* **121,** 2750–2767
3. Howe, E. N., Cochrane, D. R., Cittelly, D.M., and Richer, J. K. (2012) miR-200c targets a NF-κB up-regulated TrkB/NTF3 autocrine signaling loop to enhance anoikis sensitivity in triple negative breast cancer. *PLoS ONE* **7,** e49987
4. Buchheit, C. L., Rayavarapu, R. R., and Schafer, Z. T. (2012) The regulation of cancer cell death and metabolism by extracellular matrix attachment. *Semin. Cell Dev. Biol.* **23,** 402–411
5. Jiang, Z. F., Cristofanilli, M., Shao, Z. M., Tong, Z. S., Song, E. W., and Wang, X. J., Liao, N., Hu, X. C., Liu, Y., Wang, Y., Zeng, L., and Zhang, M. (2013) Circulating tumor cells predict progression-free and overall survival in Chinese patients with metastatic breast cancer, HER2-positive or triple-negative (CBCSG004): a multicenter, double-blind, prospective trial. *Ann. Oncol.* **24,** 2766–2772
6. Kotiyal, S., and Bhattacharya, S. (2014) Breast cancer stem cells, EMT, and therapeutic targets. *Biochem. Biophys. Res. Commun.* **453,** 112–116
7. Drury, L. J., Wendt, M. K., and Dwinell, M. B. (2010) CXCL12 chemokine expression and secretion regulates colorectal carcinoma cell anoikis through Bim-mediated intrinsic apoptosis. *PLoS ONE* **5,** e12895
8. Krawczyk, N., Meier-Stiegen, F., Banys, M., Neubauer, H., Ruckhaeberle, E., and Fehm, T. (2014) Expression of stem cell and epithelial-mesenchymal transition markers in circulating tumor cells of breast cancer patients. *Biomed. Res. Int.* **2014,** 415721
9. Sun, L., Li, T., Wei, Q., Zhang, Y., Jia, X., Wan, Z., and Han, L. (2014) Upregulation of BNIP3 mediated by ERK/HIF-1α pathway induces autophagy and contributes to anoikis resistance of hepatocellular carcinoma cells. *Future Oncol.* **10,** 1387–1398
10. Yang, J., Zheng, Z., Yan, X., Li, X., Liu, Z., and Ma, Z. (2013) Integration of autophagy and anoikis resistance in solid tumors. *Anat. Rec. (Hoboken)* **296,** 1501–1508
11. Drasin, D. J., Robin, T. P., and Ford, H. L. (2011) Breast cancer epithelial-to-mesenchymal transition: examining the functional consequences of plasticity. *Breast Cancer Res.* **13,** 226
12. Hu, Y. Y., Zheng, M. H., Zhang, R., Liang, Y. M., and Han, H. (2012) Notch signaling pathway and cancer metastasis. *Adv. Exp. Med. Biol.* **727,** 186–198
13. Kandouz, M. (2012) The Eph/Ephrin family in cancer metastasis: communication at the service of invasion. *Cancer Metastasis Rev.* **31,** 353–373

14. Qin, L. (2014) Osteopontin is a promoter for hepatocellular carcinoma metastasis: a summary of 10 years of studies. *Front Med.* **8,** 24–32
15. Warzecha, C. C., Jiang, P., Amirikian, K., Dittmar, K. A., Lu, H., Shen, S., Guo, W., Xing, Y., and Carstens, R. P. (2010) An ESRP-regulated splicing programme is abrogated during the epithelial-mesenchymal transition. *EMBO J.* **29,** 3286–3300
16. Chang, G., Wang, J., Zhang, H., Zhang, Y., Wang, C., Xu, H., Zhang, H., Lin, Y., Ma, L., Li, Q., and Pang, T. (2014) CD44 targets Na^+/H^+ exchanger 1 to mediate MDA-MB-231 cells' metastasis via the regulation of ERK1/2. *Br. J. Cancer* **110,** 916–927
17. Marzese, D. M., Liu, M., Huynh, J. L., Hirose, H., Donovan, N. C., and Huynh, K. T., Kiyohara, E., Chong, K., Cheng, D., Tanaka, R., Wang, J., Morton, D. L., Barkhoudarian, G., Kelly, D. F., and Hoon, D. S. (2015) Brain metastasis is predetermined in early stages of cutaneous melanoma by CD44v6 expression through epigenetic regulation of the spliceosome. *Pigment Cell Melanoma Res.* **28,** 82–93
18. Xu, Y., Gao, X. D., Lee, J. H., Huang, H., Tan, H., Ahn, J., Reinke, L. M., Peter, M. E., Feng, Y., Gius, D., Siziopikou, K. P., Peng, J., Xiao, X., and Cheng, C. (2014) Cell type-restricted activity of hnRNPM promotes breast cancer metastasis via regulating alternative splicing. *Genes Dev.* **28,** 1191–1203
19. Shen, H., and Weber, G. F. (2014) The osteopontin-c splice junction is important for anchorage-independent growth. *Mol. Carcinog.* **53,** 480–487
20. Vu, N. T., Park, M. A., Shultz, J. C., Goehe, R. W., Hoeferlin, L. A., Shultz, M. D., Smith, S. A., Lynch, K. W., and Chalfant, C. E. (2013) hnRNP U enhances caspase-9 splicing and is modulated by AKT-dependent phosphorylation of hnRNP L. *J. Biol. Chem.* **288,** 8575–8584
21. Goehe, R. W., Shultz, J. C., Murudkar, C., Usanovic, S., Lamour, N. F., and Massey, D. H., Zhang, L., Camidge, D. R., Shay, J. W., Minna, J. D., and Chalfant, C. E. (2010) HnRNP L regulates the tumorigenic capacity of lung cancer xenografts in mice via caspase-9 pre-mRNA processing. *J. Clin. Invest.* **120,** 3923–3939
22. West, N. W., Garcia-Vargas, A., Chalfant, C. E., and Park, M. A. (2013) OSU-03012 sensitizes breast cancers to lapatinib-induced cell killing: a role for Nck1 but not Nck2. *BMC Cancer* **13,** 256
23. Rashid, O. M., Nagahashi, M., Ramachandran, S., Dumur, C., Schaum, J., Yamada, A., Terracina, K. P., Milstien, S., Spiegel, S., and Takabe, K.(2014) An improved syngeneic orthotopic murine model of human breast cancer progression. *Breast Cancer Res. Treat.* **147,** 501–512
24. Rashid, O. M., Nagahashi, M., Ramachandran, S., Graham, L., Yamada, A., Spiegel, S., Bear, H. D., and Takabe, K. (2013) Resection of the primary tumor improves survival in metastatic breast cancer by reducing overall tumor burden. *Surgery* **153,** 771–778
25. Turimella, S. L., Bedner, P., Skubal, M., Vangoor, V. R., Kaczmarczyk, L., Karl, K., Zoidl, G., Gieselmann, V., Seifert, G., Steinhäuser, C., Kandel, E., and Theis, M. (2015) Characterization of cytoplasmic polyadenylation element binding 2 protein expression and its RNA binding activity. *Hippocampus* **25,** 630–642
26. Nairismägi, M. L., Vislovukh, A., Meng, Q., Kratassiouk, G., Beldiman, C., Petretich, M., Groisman, R., Füchtbauer, E. M., Harel-Bellan, A., and Groisman, I. (2012) Translational control of TWIST1 expression in MCF-10A cell lines recapitulating breast cancer progression. *Oncogene* **31,** 4960–4966
27. Chen, P. J., and Huang, Y. S. (2012) CPEB2-eEF2 interaction impedes HIF-1α RNA translation. *EMBO J.* **31,** 959–971
28. Hägele, S., Kühn, U., Böning, M., and Katschinski, D. M. (2009) Cytoplasmic polyadenylation-element-binding protein (CPEB)1 and 2 bind to the HIF-1α mRNA 3′-UTR and modulate HIF-1α protein expression. *Biochem. J.* **417,** 235–246
29. Kato, M., Han, T. W., Xie, S., Shi, K., Du, X., and Wu, L. C., Mirzaei, H., Goldsmith, E. J., Longgood, J., Pei, J., Grishin, N. V., Frantz, D. E., Schneider, J. W., Chen, S., Li, L., Sawaya, M. R., Eisenberg, D., Tycko, R., and McKnight, S. L. (2012) Cell-free formation of RNA granules: low complexity sequence domains form dynamic fibers within hydrogels. *Cell.* **149,** 753–767
30. Kurihara, Y., Tokuriki, M., Myojin, R., Hori, T., Kuroiwa, A., Matsuda, Y., Sakurai, T., Kimura, M., Hecht, N. B., and Uesugi, S. (2003) CPEB2, a novel putative translational regulator in mouse haploid germ cells. *Biol. Reprod.* **69,** 261–268
31. Belloc, E., and Méndez, R. (2008) A deadenylation negative feedback mechanism governs meiotic metaphase arrest. *Nature* **452,** 1017–1021
32. Belloc, E., Piqué, M., and Méndez, R. (2008) Sequential waves of polyadenylation and deadenylation define a translation circuit that drives meiotic progression. *Biochem. Soc. Trans.* **36,** 665–670
33. Bava, F. A., Eliscovich, C., Ferreira, P. G., Miñana, B., Ben-Dov, C., Guigó, R., Valcárcel, J., and Méndez, R. (2013) CPEB1 coordinates alternative 3′-UTR formation with translational regulation. *Nature* **495,** 121–125
34. Fernández-Miranda, G., and Méndez, R. (2012) The CPEB-family of proteins, translational control in senescence and cancer. *Ageing Res. Rev.* **11,** 460–472
35. Afroz, T., Skrisovska, L., Belloc, E., Guillén-Boixet, J., Méndez, R., and Allain, F. H. (2014) A fly trap mechanism provides sequence-specific RNA recognition by CPEB proteins. *Genes Dev.* **28,** 1498–1514
36. Cuenca-López, M. D., Montero, J. C., Morales, J. C., Prat, A., Pandiella, A., and Ocana, A. (2014) Phospho-kinase profile of triple negative breast cancer and androgen receptor signaling. *BMC Cancer* **14,** 302
37. Neve, R. M., Chin, K., Fridlyand, J., Yeh, J., Baehner, F. L., Fevr, T., Clark, L., Bayani, N., Coppe, J. P., Tong, F., Speed, T., Spellman, P. T., DeVries, S., Lapuk, A., Wang, N. J., Kuo, W. L., Stilwell, J. L., Pinkel, D., Albertson, D. G., Waldman, F. M., McCormick, F., Dickson, R. B., Johnson, M. D., Lippman, M., Ethier, S., Gazdar, A., and Gray, J. W. (2006) A collection of breast cancer cell lines for the study of functionally distinct cancer subtypes. *Cancer Cell* **10,** 515–527
38. Patel, N. A., Chalfant, C. E., Watson, J. E., Wyatt, J. R., Dean, N. M., Eichler, D. C., Cooper, D. R. (2001) Insulin regulates alternative splicing of protein kinase C β II through a phosphatidylinositol 3-kinase-dependent pathway involving the nuclear serine/arginine-rich splicing factor, SRp40, in skeletal muscle cells. *J. Biol. Chem.* **276,** 22648–22654
39. Cooper, D. R., Watson, J. E., Patel, N., Illingworth, P., Acevedo-Duncan, M., Goodnight, J., Chalfant, C. E., and Mischak, H. (1999) Ectopic expression of protein kinase CβII, -δ, and -ϵ, but not -βI or -ζ, provide for insulin stimulation of glucose uptake in NIH-3T3 cells. *Arch. Biochem. Biophys.* **372,** 69–79
40. Gautrey, H. L., and Tyson-Capper, A. J. (2012) Regulation of Mcl-1 by SRSF1 and SRSF5 in cancer cells. *PLoS ONE* **7,** e51497
41. Anczuków, O., Rosenberg, A. Z., Akerman, M., Das, S., Zhan, L., Karni, R., Muthuswamy, S. K., and Krainer, A. R. (2012) The splicing factor SRSF1 regulates apoptosis and proliferation to promote mammary epithelial cell transformation. *Nat. Struct. Mol. Biol.* **19,** 220–228
42. Shultz, J. C., Goehe, R. W., Wijesinghe, D. S., Murudkar, C., Hawkins, A. J., Shay, J. W., Minna, J. D., and Chalfant, C. E. (2010) Alternative splicing of caspase 9 is modulated by the phosphoinositide 3-kinase/Akt pathway via phosphorylation of SRp30a. *Cancer Res.* **70,** 9185–9196
43. Massiello, A., and Chalfant, C. E. (2006) SRp30a (ASF/SF2) regulates the alternative splicing of caspase-9 pre-mRNA and is required for ceramide-responsiveness. *J. Lipid Res.* **47,** 892–897